Environment-induced modification of spontaneous emission: Single-molecule near-field probe

Adel Rahmani

Atomic Physics Division, National Institute of Standards and Technology, Gaithersburg, Maryland 20899-8423

Patrick C. Chaumet

*Instituto de Ciencia de Materiales de Madrid, Consejo Superior de Investigaciones Científicas, Campus de Cantoblanco,
Madrid 28049 Spain*

Frédérique de Fornel

*Groupe d'Optique de Champ Proche, LPUB, CNRS UMR 5027, Faculté des Sciences Mirande, Boîte Postale 47870,
F-21078 Dijon Cedex, France*

The modification of lifetime experienced by a fluorescent molecule placed in an arbitrary environment is investigated theoretically within the framework of linear response theory. We present a complete description of the interaction of the particle with arbitrary structures on a plane substrate or inside a cavity. The theory is based on a self-consistent scattering procedure in which retardation effects and contributions from both homogeneous and evanescent modes of the electromagnetic field are included. The decay rate variations are computed and the concept of single-molecule near-field probe is discussed.

I. INTRODUCTION

Since the pioneering work of Drexhage [1], the study of fluorescence emission in finite geometries has emphasized the influence of the environment on the dynamics of the fluorescent particle [2–4]. In finite geometries, the fluorescence lifetime, or the spontaneous emission rate, differs from the free-space value because the presence of matter near the decaying particle modifies the boundary conditions imposed on the electromagnetic field [5]. If, for a fluorescent molecule, we adopt the picture of a dipole interacting with its surroundings through its field, it is the reflected field which conveys back to the molecule information concerning its environment. While this interpretation has a classical flavor, it nevertheless remains consistent with the quantum-mechanical aspects of the source-field interactions as both vacuum and radiation modes conform to the same laws and, hence, are modified in a same way when particular boundary conditions are imposed [6,7]. While exact treatments have been proposed for simple geometries [3,8], the influence of complex structures on the molecular lifetime is usually dealt with by resorting to a perturbative approach for the electromagnetic field, and/or by neglecting retardation effects, as it is the case, for instance, for a substrate with shallow roughness [9–15]. In the two-dimensional case, Bian *et al.* presented a nonperturbative treatment using the method of finite difference in time domain [16]. They computed the lifetime and the (classical) frequency shift for a dipole on a substrate as a function of its position relative to the tip of a scanning near-field optical microscope. Their calculation showed a great sensitivity of the dynamics of the dipole with respect to its position beneath the tip consistent with experimental observations [17–19]. Another numerical study of lifetime modification was presented by Girard *et al.* [20], however, these authors based their work on a misconception of the coupling of a two level atom with radiation, as they ignored the fundamental relation between the free-space decay rate of spontaneous emission and the atom polarizability, leading to an unsound model. The three-dimensional problem was addressed by Novotny who studied the influence of a scanning near-field optical microscope tip, represented by an aluminum disk-shaped object, on the fluorescence lifetime of a dipole lying on a substrate [21]. His calculation, using a semianalytical method derived from the multiple multipole method [22], showed that the orientation of the dipole was critical, especially when the dipole was located close to the rim of the object.

The great sensitivity of a fluorescent molecule to its environment, makes it an interesting candidate for an elementary near-field probe [23–27]. In order to assess the potential of such a single-molecule probe, it is crucial to describe properly the coupling of the molecule to its environment. The purpose of this work is thus to study, in three dimensions, the modification of the fluorescence decay rate of a molecule by arbitrary structures, including ones too large to be used in a Born-type perturbative approach. The formalism presented here is based on a knowledge of the dynamical electromagnetic response of a plane surface or cavity to both homogeneous and evanescent modes of the field. The dressed, retarded field susceptibility pertaining to the environment is derived through a self-consistent procedure. The decay rate of the molecule is then computed according to linear response theory. Our paper is organized as follows. Using linear response theory, we relate in Sec. II the spontaneous emission rate to the field susceptibility. Using the theory of Agarwal [28,29], we then derive the exact retarded field susceptibility tensor associated with a surface (interface between two media). The relevant quantity in the problem of spontaneous emission is the field correlation function. Since this correlation function can be related to the field linear susceptibility through the fluctuation-dissipation theorem [28], this approach, while rigorously quantal, avoids an explicit quantization of the field. In Sec. III, we insert this tensor into the self-consistent procedure of the coupled di-

pole method (CDM) and compute the dressed field-susceptibility accounting for many-body interactions between the fluorescent particle, a plane surface, and an arbitrary object deposited on it, and we compute the decay rate for a transition dipole moment with arbitrary orientation. Since our calculation includes retardation effects, we are able to treat the case of extended structures. Both lossless dielectric and absorbing materials (dielectric or metallic) are considered. Section IV is devoted to the application of the CDM to the study of decay rate modification near microstructures placed on a plane substrate. Several examples are considered (dielectrics and metals) to foster understanding of the interactions between the molecular source and the environment. Particularly, we illustrate the different coupling mechanisms involved in the alteration of the dynamics of the molecular source. The molecular dynamics is studied further in Sec. V, where the possibility of a single-molecule near-field probe is demonstrated. Finally, our conclusions are presented in Sec. VI.

II. EXACT RETARDED FIELD SUSCEPTIBILITY OF A FLAT SURFACE

Since Purcell's prediction [5], the study of the influence of finite geometries on spontaneous emission gave rise to a large body of work, where both the viewpoint of classical [1,3,4] and quantum [26–32] electrodynamics were adopted (see the recent reviews by Haroche [6] and Barnes [33]). For our purpose, the choice of the formalism (classical versus quantum-mechanical) to describe the particle has little consequence on the final conclusion, at least as far as the decay rate, or its inverse the lifetime, is concerned (level shifts are discussed in the Appendix). Note that this is true because we consider a weak coupling regime (irreversible decay). We might either consider an excited two-level atom and compute its electric-dipole transition rate from the excited to the ground state (separated by an energy $\hbar\omega$) according to Fermi's golden rule, or a classical oscillating dipole whose oscillations (at frequency ω) are damped or enhanced by the field reflected by the environment. Both approaches lead to the same result [26]. We will use the shorthand ''dipole'' to identify the decaying particle, and whenever it will be appropriate, we shall exploit the intuitive character of the classical interpretation. In linear-response theory, the (linear) field susceptibility is the response of the electromagnetic field to an elementary excitation [28,34–36]. Let the dipole $\boldsymbol{\mu}(\mathbf{r}_0,\omega)$ be located at $\mathbf{r}_0=(x_0,y_0,z_0)$, $z_0>0$ in vacuum (permittivity $\epsilon_0=1$) above a substrate [permittivity $\epsilon_s(\omega)$ for $z<0$]. The electric field at position $\mathbf{r}=(x,y,z)$ above the interface is given by

$$\mathbf{E}(\mathbf{r},\omega)=\mathbf{T}(\mathbf{r},\mathbf{r}_0,\omega)\boldsymbol{\mu}(\mathbf{r}_0,\omega), \qquad (1)$$

where $\mathbf{T}$, the total field-susceptibility tensor, consists of $\mathbf{F}$, the free-space [37] and $\mathbf{S}$, the surface field susceptibilities:

$$\mathbf{T}(\mathbf{r},\mathbf{r}_0,\omega)=\mathbf{F}(\mathbf{r},\mathbf{r}_0,\omega)+\mathbf{S}(\mathbf{r},\mathbf{r}_0,\omega). \qquad (2)$$

To derive the damping rates, we need to find the *dissipative* part of the force acting upon the dipole. This damping force

consists of the part of the electric field which is $\pi/2$ out-of-phase with respect to the dipole's oscillations. From linear-response theory we can write the normalized damping (decay) rate as

$$\left(\frac{\Gamma}{\Gamma_0}\right)_l=1+\frac{3q}{2k_0^3}\mathrm{Im}[S_{ll}(\mathbf{r}_0,\mathbf{r}_0,\omega)], \qquad (3)$$

where $\mathrm{Im}(X)$ is the imaginary part of X, $k_0=2\pi/\lambda$ (λ is the wavelength, in vacuum, of the electric dipole transition), and q denotes the intrinsic quantum yield of the molecule. For simplicity we will take $q=1$. The subscript l stands for one of the three Cartesian coordinates x,y,z. The quantity Γ_0 is the free-space decay rate, it includes the contribution from $\mathbf{F}$ so that only the surface contribution remains in the expression of the *normalized* decay rate [Eq. (3)]. The next step consists in deriving the surface field susceptibility $\mathbf{S}$ through a rigorous treatment of the boundary-value problem at the interface. Starting from the field emitted by a dipole in free space, one must perform a plane wave expansion of the field and consider the interaction of each mode (either homogeneous or evanescent) with the surface [28]. At the end one can write the components of the surface field susceptibility as [26]

$$S_{xx}(\mathbf{r},\mathbf{r}_0,\omega)=\frac{i}{2}\left(\int_0^{k_0}-\int_0^{i\infty}\right)dw_0\{[\Delta_p w_0^2-\Delta_s k_0^2]$$
$$\times e^{iw_0(z+z_0)}J_0(R\sqrt{k_0^2-w_0^2})-\cos(2\phi)$$
$$\times[\Delta_p w_0^2+\Delta_s k_0^2]e^{iw_0(z+z_0)}J_2(R\sqrt{k_0^2-w_0^2})\}, \qquad (4)$$

$$S_{xy}(\mathbf{r},\mathbf{r}_0,\omega)=-\frac{i}{2}\sin(2\phi)\left(\int_0^{k_0}-\int_0^{i\infty}\right)dw_0[\Delta_p w_0^2+\Delta_s k_0^2]$$
$$\times e^{iw_0(z+z_0)}J_2(R\sqrt{k_0^2-w_0^2}), \qquad (5)$$

$$S_{xz}(\mathbf{r},\mathbf{r}_0,\omega)=-i\cos\phi\left(\int_0^{k_0}-\int_0^{i\infty}\right)dw_0\sqrt{k_0^2-w_0^2}$$
$$\times J_0(R\sqrt{k_0^2-w_0^2})e^{iw_0(z+z_0)}w_0\Delta_p, \qquad (6)$$

$$S_{zz}(\mathbf{r},\mathbf{r}_0,\omega)=-i\left(\int_0^{k_0}-\int_0^{i\infty}\right)dw_0(k_0^2-w_0^2)$$
$$\times J_0(R\sqrt{k_0^2-w_0^2})e^{iw_0(z+z_0)}\Delta_p, \qquad (7)$$

where Δ_p and Δ_s are the Fresnel coefficients for p-polarized (transverse magnetic) and s-polarized (transverse electric) homogeneous or evanescent waves falling onto the interface. The distance $R=\sqrt{(x-x_0)^2+(y-y_0)^2}$, ϕ is the angle defined by $\cos\phi=(x-x_0)/R$, and $w_0^2=k_0^2-k_x^2-k_y^2$. The functions J_0 and J_2 are Bessel functions of the first kind [38]. The other components of this tensor can be deduced by symmetry. The respective contributions from homogeneous and evanescent modes of the field are readily identified by looking at the domains of integration of the two integrals. The

decay rates can then be computed by inserting the expression of **S** in Eq. (3). Here both homogeneous and evanescent parts of the surface field susceptibility are likely to contribute to the decay rate, unlike the free-space case where evanescent modes of the field are absent from the dissipative process [39].

III. MANY-BODY INTERACTIONS AND SELF-CONSISTENT FIELD SUSCEPTIBILITY

In the preceding section we considered the case of a dipole above a bare surface. Let us now consider the situation where an object is present near or on the surface. In such a case, the response of the environment to the dipole is not given by **S** anymore. One possible way to describe the influence of the object on the scattering process is to use the coupled dipole method [40] where the object is described as a collection of N polarizable subunits with dynamical polarizabilities $\alpha_i(\omega)$ located at positions $\mathbf{r}_i$ ($i=1,N$) on a cubic lattice. Let the molecule be located at $\mathbf{r}_0$, the self-consistent field susceptibility associated with the dressed surface is thus given by a set of N linear equations

$$\mathbf{S}_D(\mathbf{r}_i,\mathbf{r}_0,\omega)=\mathbf{F}(\mathbf{r}_i,\mathbf{r}_0,\omega)+\mathbf{S}(\mathbf{r}_i,\mathbf{r}_0,\omega)+\sum_{j=1}^{N}\,[\mathbf{F}(\mathbf{r}_i,\mathbf{r}_j,\omega)$$
$$+\mathbf{S}(\mathbf{r}_i,\mathbf{r}_j,\omega)]\alpha_j(\omega)\mathbf{S}_D(\mathbf{r}_j,\mathbf{r}_0,\omega), \qquad (8)$$

for $i=1,N$. We shall assume that the optical properties of the object is isotropic so that the polarizability is scalar. The dynamical polarizability of each unit of discretization is given by [41–43]

$$\alpha_i(\omega)=\frac{\alpha^{\text{CM}}(\omega)}{1-(2/3)ik_0^3\alpha^{\text{CM}}(\omega)}, \qquad (9)$$

where $\alpha^{\text{CM}}(\omega)$ is the expression for the polarizability derived from the Clausius-Mossotti relation

$$\alpha^{\text{CM}}(\omega)=\frac{3d^3}{4\pi}\frac{\epsilon(\omega)-1}{\epsilon(\omega)+2}, \qquad (10)$$

with $\epsilon(\omega)$ the permittivity of the object and d the lattice spacing of the discretization.

Since the decay rate of the dipole is related to the dissipative part of the field susceptibility tensor at the position of the dipole, we seek to find $\mathbf{S}_D(\mathbf{r}_0,\mathbf{r}_0,\omega)$. After solving the self-consistent equation (8) for $\mathbf{S}_D(\mathbf{r}_i,\mathbf{r}_0,\omega)$ ($i=1,N$), we can write [26,27]

$$\mathbf{S}_D(\mathbf{r}_0,\mathbf{r}_0,\omega)=\mathbf{S}(\mathbf{r}_0,\mathbf{r}_0,\omega)+\sum_{i=1}^{N}\,[\mathbf{F}(\mathbf{r}_0,\mathbf{r}_i,\omega)$$
$$+\mathbf{S}(\mathbf{r}_0,\mathbf{r}_i,\omega)]\alpha_i(\omega)\mathbf{S}_D(\mathbf{r}_i,\mathbf{r}_0,\omega),$$
$$(11)$$

where the free-space term $\mathbf{F}(\mathbf{r}_0,\mathbf{r}_0,\omega)$ has been discarded because the contribution of this self-term is included in the free-space decay rate.

A convenient way to understand the physical content of Eq. (11) is to think in terms of electric field [44]. To do so we introduce the dipole moment and cast Eq. (11) in the form

$$\mathbf{S}_D(\mathbf{r}_0,\mathbf{r}_0,\omega)\boldsymbol{\mu}(\mathbf{r}_0,\omega)$$
$$=\mathbf{S}(\mathbf{r}_0,\mathbf{r}_0,\omega)\boldsymbol{\mu}(\mathbf{r}_0,\omega)$$
$$+\sum_{i=1}^{N}\,[\mathbf{F}(\mathbf{r}_0,\mathbf{r}_i,\omega)+\mathbf{S}(\mathbf{r}_0,\mathbf{r}_i,\omega)]\alpha_i(\omega)$$
$$\times\mathbf{S}_D(\mathbf{r}_i,\mathbf{r}_0,\omega)\boldsymbol{\mu}(\mathbf{r}_0,\omega). \qquad (12)$$

The right-hand side of Eq. (12) can be decomposed as follows.

The term $\mathbf{S}(\mathbf{r}_0,\mathbf{r}_0,\omega)\boldsymbol{\mu}(\mathbf{r}_0,\omega)$ represents the radiation reaction effect caused by the interaction of the molecule with its own field reflected by the substrate.

The term $\mathbf{S}_D(\mathbf{r}_i,\mathbf{r}_0,\omega)\boldsymbol{\mu}(\mathbf{r}_0,\omega)$ represents the self-consistent field induced by the molecule at the position of the ith polarizable element of the object (this element being coupled to the $N-1$ others).

Finally, as a whole, the sum in Eq. (12) represents the reaction of all the elements of the object, self-consistently coupled to the substrate, on the molecule.

The spontaneous emission rates are still given by Eq. (3) except that the field susceptibility of the bare surface (**S**) is now to be replaced by the field susceptibility of the dressed surface ($\mathbf{S}_D$).

IV. SPONTANEOUS-EMISSION RATES

We shall now use the theory described in the preceding sections to compute the decay rate of a fluorescent molecule. The configuration is the following. The molecule is located in vacuum at a distance z_0 from a surface [(x,y) plane]. The structures considered are parallelepipeds with square base $b\times b$ and height h. Other shapes can be considered (see, for instance, Refs. [43–47]) but because of the cubic symmetry of the CDM discretization procedure, for an equal volume, they would require a larger number of elements to be described properly. Moreover this choice will allow us to study the effect of sharp edges and corners on the molecular fluorescence lifetime. In the following we will always plot the normalized decay rate (inverse of the normalized lifetime, the normalization being performed with respect to the molecule in vacuum) as a function of the molecule position in the plane $z=z_0$. Except for Fig. 2 the parallel dipole is chosen to be oriented along x. The values of the permittivity for metals are taken from Ref. [48].

A. Dielectrics

We first consider the case of a dielectric substrate ($\epsilon_s=2.25$), the wavelength of the transition is 612 nm. Deposited on the substrate are three dielectric parallelepipeds ($\epsilon=2.25$) with dimensions $h=50$ nm and $b=100$, 200, and 250 nm, respectively (Fig. 1). This example will serve to illustrate an important feature which stems from the near-
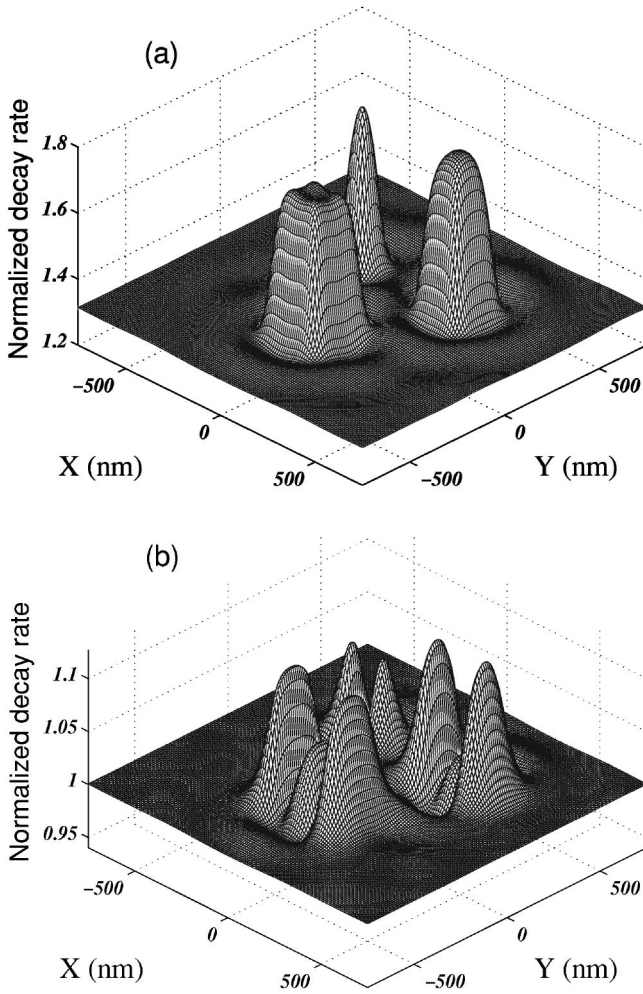
FIG. 1. Normalized decay rate above three dielectric objects (see text) placed on a dielectric substrate ($\epsilon = \epsilon_s = 2.25$, $\lambda = 612$ nm, $d = 25$ nm, $z_0 = 90$ nm). (a) Dipole moment along z. (b) Dipole moment along x.
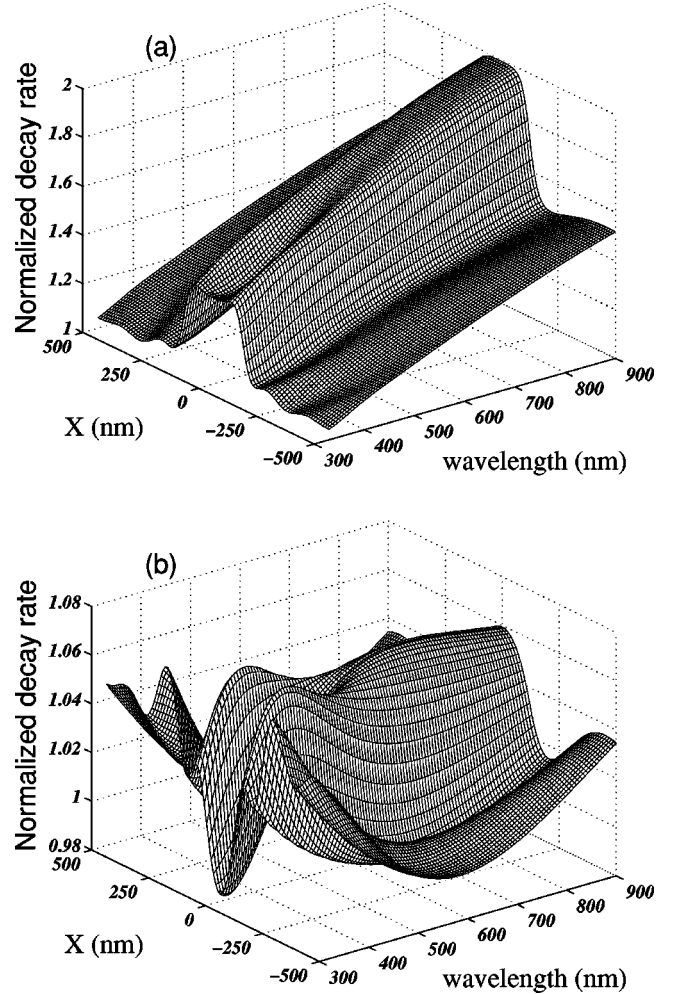

FIG. 2. Normalized decay rate above a dielectric object ($h = 50$ nm, $b = 250$ nm, $d = 25$ nm, $\epsilon = 2.25$, $z_0 = 90$ nm), on a dielectric substrate ($\epsilon_s = 2.25$) as a function of the position along the x axis ($y = 0$) and of the wavelength of emission. The dipole moment is along z (a) or y (b).

field nature of the interaction between the molecule and its environment. In this regime the role of evanescent modes of the field is essential [49]. Indeed, it is through these modes that the molecule couples to the high spatial frequencies (edges, corners) of the objects. On the other hand, the fast damping associated with these modes entails that the larger the distance between the molecule and the object, the softer the spatial variations of the lifetime, because the highly evanescent modes of the field that would interact with the sharpest features of the object decay so fast that they vanish before they could be scattered (or absorbed in the material in the case of a lossy material). Moreover, the orientation of the molecule dipole moment influences strongly the decay rate. The variations observed on Fig. 1(a), for the perpendicular (with respect to the substrate) orientation of the dipole moment of the molecule, reflects more closely the actual shape of the adsorbed structure as the object gets larger. The case of a parallel dipole (along x) is different as the rotational symmetry around the z axis is broken and boundary effects prevail [Fig. 1(b)]. The strong edge effect is a consequence of the normal component of the electric field being discon-

tinuous (see Ref. [26]). Particularly, this effect is responsible for an inhibition ($\Gamma/\Gamma_0 < 1$) of spontaneous emission above the smallest pad. As the pad gets larger, the edges recede away from each other and the decay rate above the center of the pad tends towards that of a molecule located $z_0 - h$ away from a bare surface. The sensitivity of the decay rate on the emission wavelength is illustrated further on Fig. 2. Note that this is a purely ''geometrical'' effect as we assume that the permittivity of the object is constant over the whole spectrum ($\epsilon = 2.25$). Figure 2(a) shows the variation of the perpendicular decay rate along direction x, as a function of the wavelength of the light emitted by the dipole, for an object with $h = 50$ nm and $b = 250$ nm, and a distance dipole substrate of $z_0 = 90$ nm. As we mentioned, for any given distance, the ability of the dipole to ''see'' the spatial variation of the object depends on the wavelength of the emission; the larger the wavelength and the more uniform the decay rate over the object. One can also note that the substrate contribution to the decay rate increases with the wavelength. This is a reflection of the growing importance of frustration of
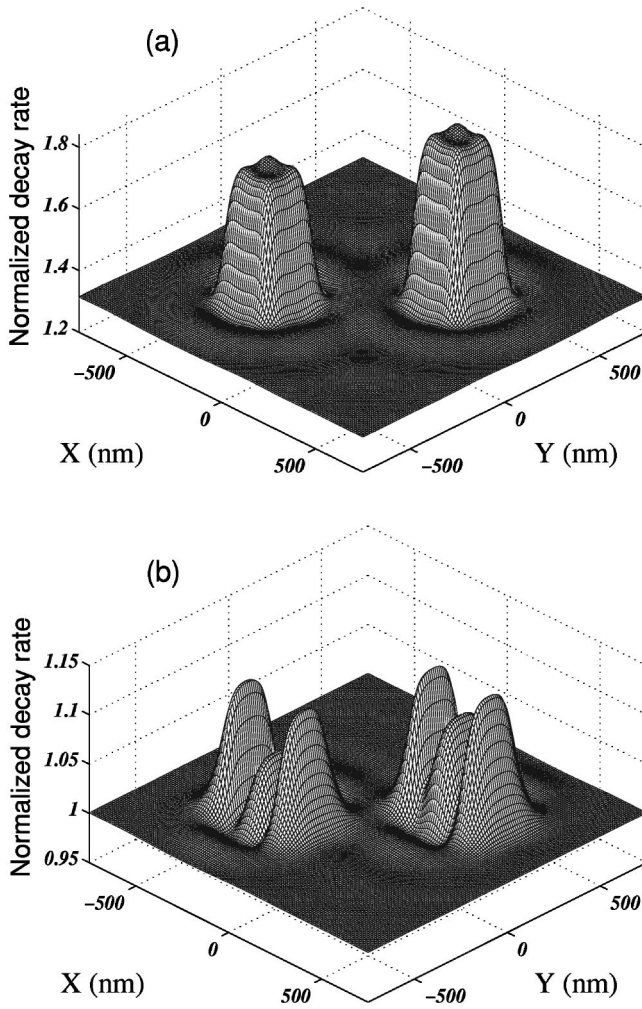
FIG. 3. Normalized decay rate above two dielectric objects (left: $\epsilon = 2.25$ and right: $\epsilon = 2.25 + 0.1i$) placed on a dielectric substrate ($\epsilon_s = 2.25$, $\lambda = 612$ nm, $d = 25$ nm, $z_0 = 90$ nm). (a) Dipole moment along z. (b) Dipole moment along x.

evanescent waves as z_0/λ decreases. This near-field effect is somewhat more difficult to observe in the case of a parallel dipole [Fig. 2(b)] because, for this orientation, it is concealed by the reflection of the propagating ($\sim 1/r$) component of the field.

We shall now consider an absorbing dielectric. The consequence of absorption is illustrated on Fig. 3. The two objects are identical except for the imaginary part of the permittivity. Note how retardation makes the decay rate oscillates away from the parallelepipeds. Aside from orientational features, the effect of absorption is to increase the decay rates. Indeed, recall that the normalized decay rate represents the losses of the molecule; absorption in the material provides the molecule with an additional decay channel. Unlike the mechanism of frustration, absorption affects all the evanescent modes of the field emitted by the decaying particle; as a result this decay channel dominates the molecular losses at very short distances. As the dipole gets closer to a lossless medium, its lifetime tends towards a finite value because the mechanism of frustration affects only those eva-

nescent modes whose component of the wave vector parallel to the interface is between k_0 and $k_0\sqrt{\epsilon}$. The case of an absorbing medium is different. The closer the dipole to the absorbing surface and the more evanescent modes reach the material and are absorbed which makes the lifetime go to zero (of course, the lifetime does not become zero because the present description in terms of dipole and flat surface would actually become invalid for distances smaller than a few Å).

B. Metals

If at first we disregard the object, the influence of a metallic surface on the decay rate of the dipole will significantly depend on the wavelength of the transition, and since we are in a near-field regime, on the distance between the molecule and the surface. The interaction of a dipole with a flat metallic surface is addressed in detail in Refs. [3,4,9,27], and references therein, and we will here merely underline the major features. First, an important contribution to the decay rate arises from the excitation of surface plasmon on the metallic surface. It can be shown that this contribution might prevail over any other process even at fairly large (a few hundreds nm) distances from the surface [50]. For small separations, absorption dominates; the coupling to surface modes is, however, more efficient when the wavelength of the dipole transition is close to the surface plasmon wavelength. One can also note that when the dipole is close to the surface, retardation becomes negligible and the perpendicular decay rate is twice the parallel decay rate as expected [limit $k_0 = 0$ in Eqs. (4) and (7)]. In summary, the case of a metallic substrate is a combination of reflection, frustration, absorption, and surface mode excitation [27].

Thus, when metals are involved, the decay rate variations will strongly depend on the wavelength of the dipole transition. Since the purpose of this work is to give a general picture of the near-field coupling of a decaying particle to its environment, in the following, we shall restrict ourselves to a few situations that will help us illustrate the various physical processes involved. Let us now consider the same objects as on Fig. 3, but located on a gold substrate. The decay rate maps are shown on Fig. 4. The differences in the influence of the two objects on the molecule are attenuated by the presence of the gold substrate. While the overall variation of the decay rate for a perpendicular dipole [Fig. 4(a)] strongly resembles the one observed for a dielectric substrate, the situation is quite different for the parallel dipole [Fig. 4(b)]. The presence of the metallic substrate leads, for the emission wavelength considered, to a strong damping when the molecule is above one of the objects.

Actually, when the molecule is above one of the objects, the coupling mechanism can be understood with a simple model. The width of the objects is large enough to allow the decay rate to get fairly close to the limit value it would have, had the molecule been placed above a multilayered structure composed of a gold substrate and a dielectric layer of thickness h. To compute the decay rate in such an environment, we replace the Fresnel coefficients appearing in Eqs. (4)–(7) by those of a multiple interface system [51]. We can then study the evolution of the decay rates for a molecule located
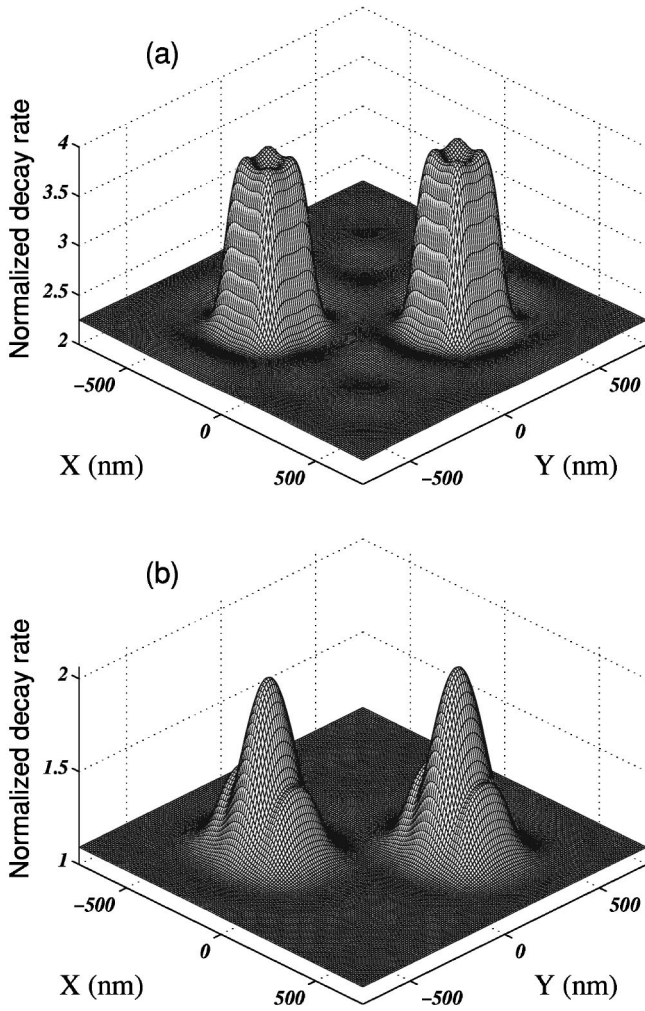
(a)

(b)

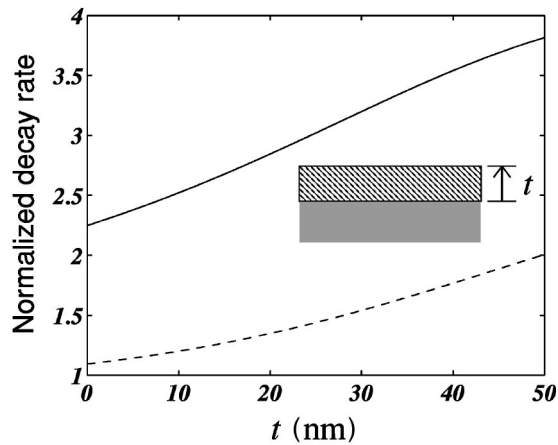FIG. 4. Same as Fig. 3 but with a substrate of gold.

(a)

(b)

FIG. 6. Normalized decay rate above two dielectric objects (left: $\epsilon = 2.25$ and right: $\epsilon = 5$) placed on a gold substrate ($\lambda = 520$ nm, $d = 25$ nm, $z_0 = 90$ nm). (a) Dipole moment along z. (b) Dipole moment along x.

FIG. 5. Rate evolution for a multilayer system as a function of the thickness (t) of a dielectric layer ($\epsilon = 2.25, \lambda = 612$ nm) deposited on top of a gold substrate. The distance between the dipole and the substrate is 90 nm. Solid line, dipole moment perpendicular to the surface, dashed line, dipole moment parallel.
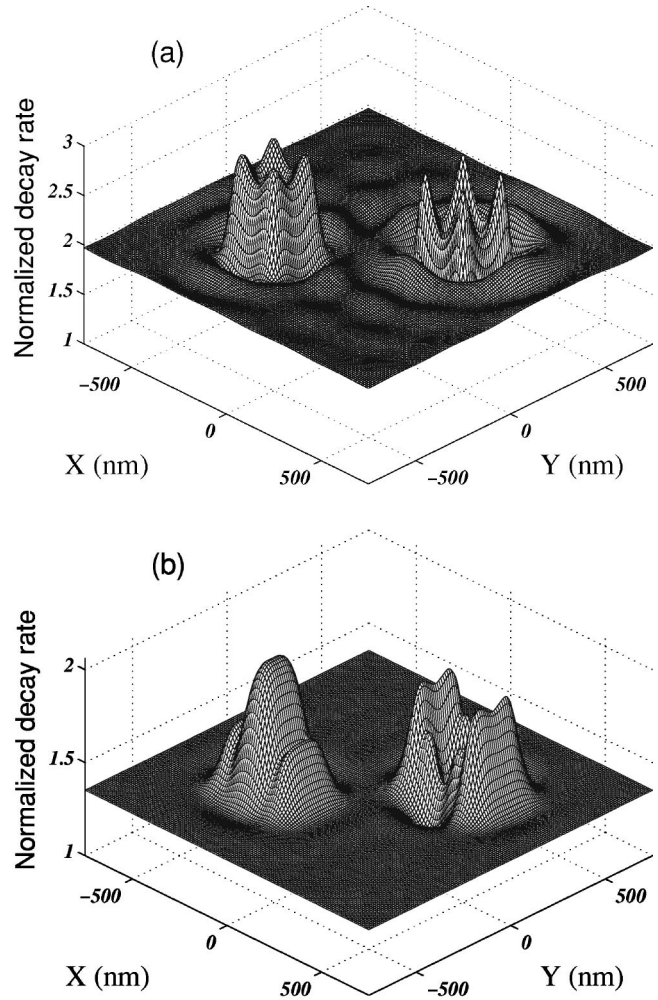
at distance z_0 from the gold substrate, as a dielectric layer ($\epsilon = 2.25$) is grown on top of it (Fig. 5). It becomes clear that the strong damping experienced by the molecule over the parallelepipeds comes from this multilayer effect. Note that, as we shall see on the next example, the enhancement of the decay rate, as the dielectric layer is grown, does not translate a mere effect of frustration of the near field of the dipole as the thickness of the dielectric increases.

The previous example shows that a small difference between the imaginary parts of the permittivities of the two structures has little consequence on the decay rate of the molecule; at least for the distances we just considered. In order to have a better insight let us consider a case where the difference between the permittivities of two nonabsorbing objects is larger (2.25 and 5). The substrate is still gold, and the wavelength of the transition is chosen to be 520 nm. The variations of the decay rates for this case are shown on Fig. 6. The decay rate variations are now significantly different for the two structures. Particularly, one can see that the interaction of the molecule with the objects does not amount to a mere mechanism of frustration of the near-field of the mol-
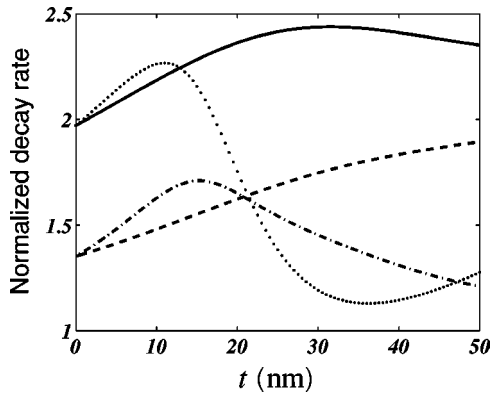
FIG. 7. Same as Fig. 5 but with $\lambda = 520$ nm. Solid line: $\epsilon = 2.25$, dipole along z. Dot-dashed line: $\epsilon = 2.25$, dipole along x. Dotted line: $\epsilon = 5$, dipole along z. Dashed line: $\epsilon = 5$, dipole along x.

ecule. The decay rate is more enhanced over the parallelepiped with the *lowest* permittivity. Once again, this feature can be explained by considering a multilayer configuration (Fig. 7). Despite its simplicity, this simple model is extremely valuable in that it provides us with an easy way to understand the behavior of the molecule above the objects. However, one should bear in mind that the good agreement between the value of the decay rates when the molecule is centered above one object, and the one given by a simple (infinite) multilayer model will hold as long as the lateral dimensions of the object are large enough.

The next two cases will allow us to illustrate further the sensitivity to the environment of the molecular response. For a transition wavelength of 520 nm, we consider the silver/gold pair. In the first case an object made of gold is placed on a silver substrate (Fig. 8). In the second case, the roles of the two metals are exchanged (Fig. 9). From this single example, it is obvious that not only the magnitude, but also the qualitative variations of the decay rates depend drastically on the nature of the materials forming the environment of the
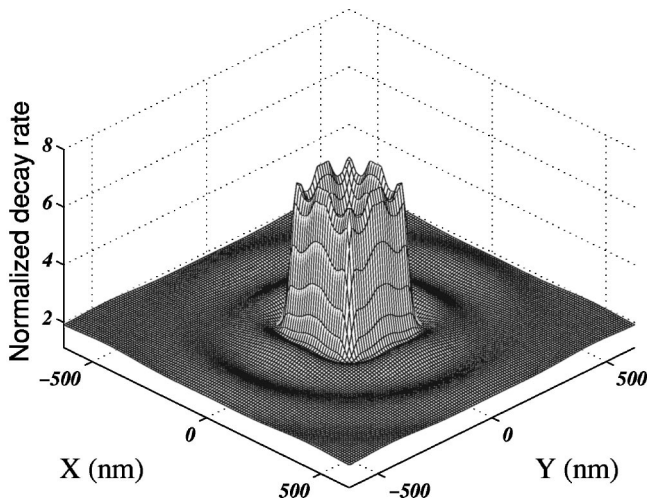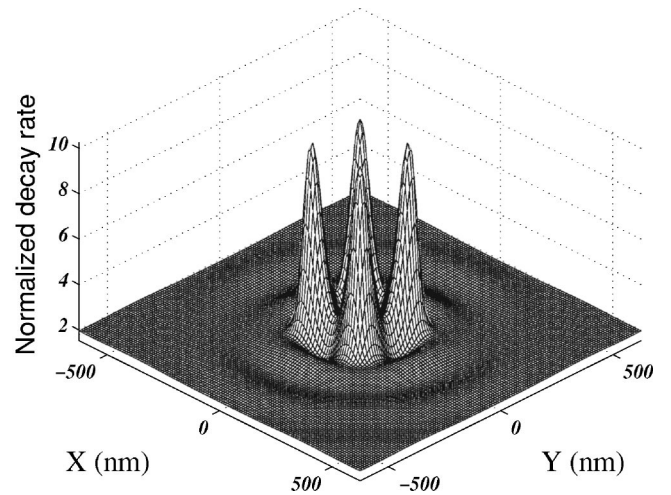

FIG. 9. Normalized decay rate above a silver structure ($\lambda = 520$ nm, $d = 12.5$ nm, $z_0 = 90$ nm) placed on a gold substrate. Dipole moment along z.

molecule (see also Ref. [27]). Nevertheless, a general conclusion may be drawn. Spatially localized perturbations of the environment of the molecule can couple to the evanescent modes pervading the near field of the molecule. Hence, although these evanescent modes do not contribute to the dissipation of energy for a molecule in free space [39], their scattering by the environment provides the molecule with an additional decay channel (in addition to frustration, absorption, and reflection).

V. SINGLE-MOLECULE NEAR-FIELD PROBE

In the preceding section we saw the great diversity of the molecular response; the way the molecule couples to its environment depends on the geometry as well as on the nature of the environment. On the one hand, such diversity might be construed as a hindrance for an easy correspondence between the environment and the molecular response; a correspondence crucial if the molecule were to be used as a near-field probe. On the other hand, the fact that different objects yield radically different molecular responses can be viewed as an asset for two different material could, at least in principle, be unambiguously distinguished. To assess the potential for imaging of a single-molecule probe in a somewhat more transparent way, let us consider a structure of no particular symmetry. We are interested in the ability for the molecular decay rate to reflect the symmetry of the structure. For simplicity we model the structure by a single layer of 410 coupled dipoles. The height of the structure is 20 nm and its permittivity is 2.25 (same as the permittivity of the substrate). The probe molecule is scanned over the structure at constant height 40 nm. If the scanning distance were to be shortened, the size of the dipoles forming the structure would simply have to be reduced. Moreover, we suppose that the molecule is attached to a dielectric material with permittivity 2.25, which consists of a semi-infinite medium occupying the half space $z \geq 40.5$ nm. This geometry corresponds to a worst case scenario since for any material of finite lateral extend, multiple scattering would be less important. The de-

FIG. 8. Normalized decay rate above a gold structure ($\lambda = 520$ nm, $d = 12.5$ nm, $z_0 = 90$ nm) placed on a silver substrate. Dipole moment along z.
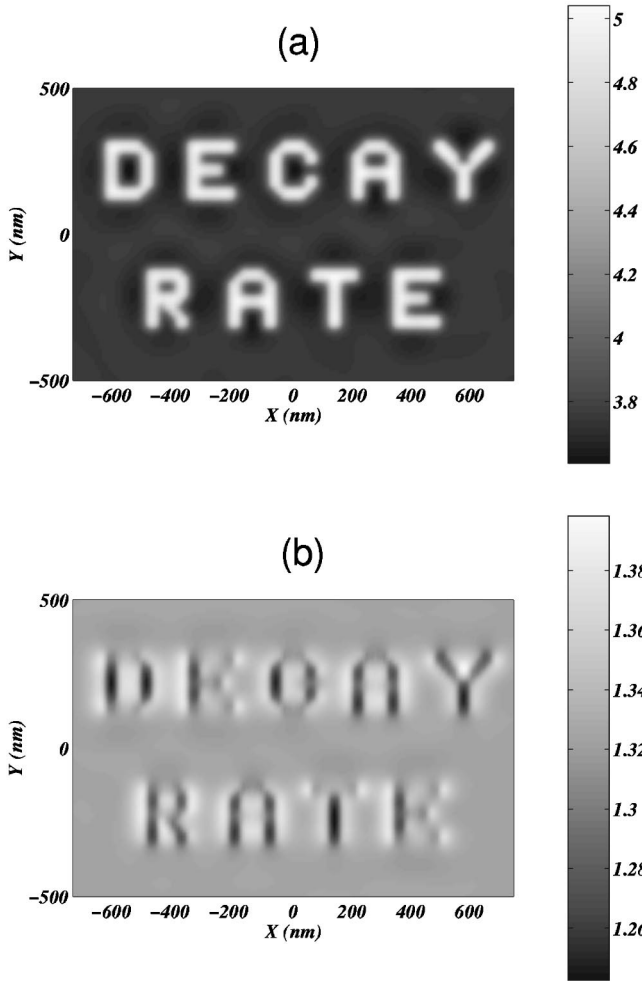
FIG. 10. Single-molecule near-field image ($\lambda = 488$ nm) in a cavity configuration (see text) for a dielectric substrate ($z_0 = 40$ nm). The dipole moment is along z (a) or x (b).

FIG. 11. Same as Fig. 10 but for a gold substrate.

cay rate is computed by deriving the self-consistent field susceptibility of a dressed cavity [26,27] in a fashion similar to the one described in Sec. II, but with the surface now replaced by a three-media junction. The results presented on Fig. 10 show that the decay rate variations are strongly correlated to the actual shape of the sample only in the case of a molecule transition moment oriented along the z axis. This is a logical result as, for the perpendicular (z) case the molecular probe response is symmetric in the scanning plane, while in the parallel (x) case, the true features of the sample are concealed by strong edge effects which are a reflection of the fact that the normal component of the electric field is discontinuous across an interface. Hence, in the case of a perpendicular dipole moment, there exists a rather obvious correspondence between the decay rate variations and the actual shape of the sample. The same applies in the case of a metallic substrate (Fig. 11). This correspondence holds for more extended structures [27]. Hence, provided that the dipole moment of the probe is oriented perpendicular to the substrate, a single molecule could in principle act as a localized near-field probe. On the other hand, for parallel orientation, one obtains a probe sensitive to the frontiers between do-
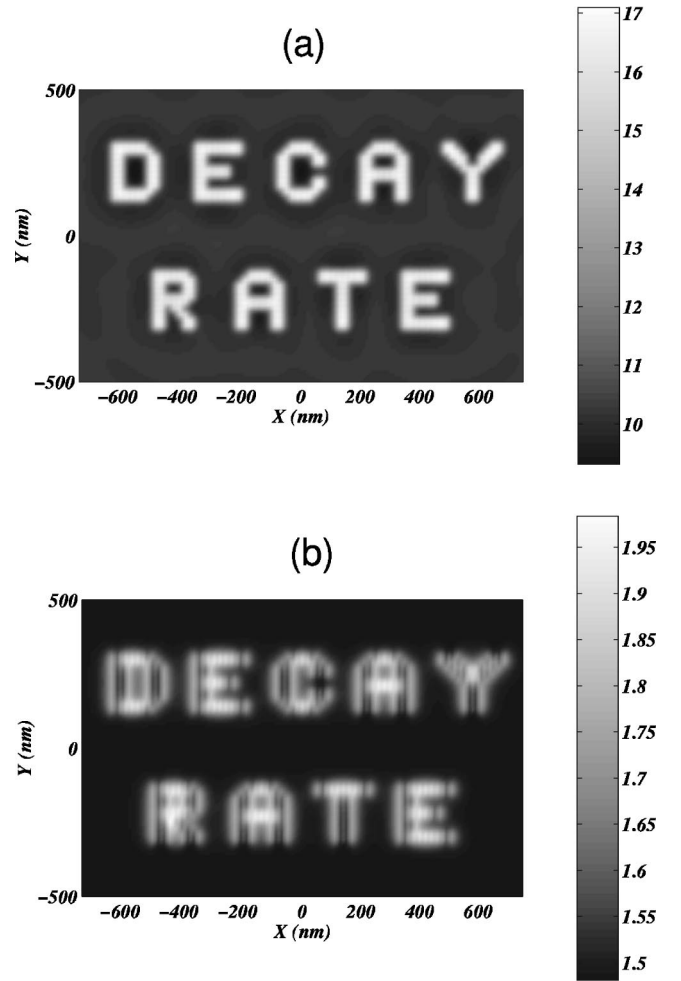
mains with different permittivities. One should also note that since the dynamics of the molecular probe depends on the optical properties of the environment, the decay rate would also be affected if the molecule were scanned over a flat sample (no topographic features) exhibiting a strong optical contrast.

VI. CONCLUSION

We have presented a theoretical model for the study of near-field modification of spontaneous emission. The coupled dipole method (CDM), allied with a rigorous derivation of the self-consistent electric field linear susceptibility which includes retardation effects, allowed us to address the electromagnetic coupling between an elementary source (molecule or atom) and its environment. Our approach is not restricted to a perturbative scattering regime or to a particular type of environment. Once the electromagnetic response (susceptibility) of a simple environment is determined, in our case a substrate or a cavity, the flexibility of the CDM allows one to consider general structures.

Using this approach, we have computed the decay rates for a single molecule represented by an oscillating dipole, as a function of its position above various structures deposited

on a substrate. We have considered both the dielectric and the metallic case. While the details of the molecular response depend on the very nature of its environment, we have shown that the orientation of the dipole moment of the probe is crucial as in the parallel case (dipole in the scanning plane) the near-field decay rate map is dominated by features stemming from the discontinuity of the normal component of the electric field across interfaces [26]. Also, the scattering of the evanescent modes by sharp features of the sample provides the molecule with an additional decay channel. Accordingly, the decay rates are enhanced around corners or sharp features in general. This result is consistent with previous experimental and theoretical investigations [16–19,21]. For a better assessment of the potential of a single molecule for use as a near-field probe, we placed the molecule in a cavity, thus maximizing multiple scattering, and we considered a geometrically complex sample. This example demonstrated that, provided that the probe's dipole moment is conveniently oriented (in the cases considered in this paper this corresponds to a moment perpendicular to the scanning plane), the decay rate near-field map, is indeed strongly correlated to the actual geometry of the sample. Of course, in the case of a sample composed of several materials whose optical responses are radically different, especially in the case of metals, such a simple correspondence between decay rate variations and sample geometry is likely to be lost. As in any near-field interaction, the distance between the probe and the sample will also influence the decay rate variations. As the distance decreases (increases), the identification of the sample through its near-field signature on the decay rate of the probe becomes easier (more difficult). More detailed studies are presented in Ref. [27].

To conclude, let us state that the theoretical validation of the concept of a single-molecule near-field probe should not occult the difficulties encumbering the road to an experimental realization of such a single-molecule near-field probe (some of these aspects are discussed in Refs. [27,15]). However, the main idea behind an efficient near-field probe is localization and while using a single-molecule might prove to be difficult, if one could gather several of these molecules in a small volume, coherent coupling between these molecules could well permit the realization of a multimolecular probe without compromising the near-field sensitivity. Yet another possibility might be to isolate spectrally a molecule embedded in a host crystal by taking advantage of the inhomogeneous spectral broadening as was done recently to create a single molecule near-field source [52]. Also, let us mention that as pointed out by Agarwal [53], the effect of the environment on the field can be viewed as the breaking of the isotropy of the mode distribution of the vacuum state of the field. This is another way of explaining the dependence of the decay rate on the orientation of the transition moment of the molecule. However, as Agarwal demonstrated, this anisotropy of the vacuum also has the interesting property that it can lead to interferences in the decay from two close lying states to a common state, even if the dipole moments of the two states are orthogonal. Such interference effects could, in principle, also be studied with a single-molecule near-field probe.
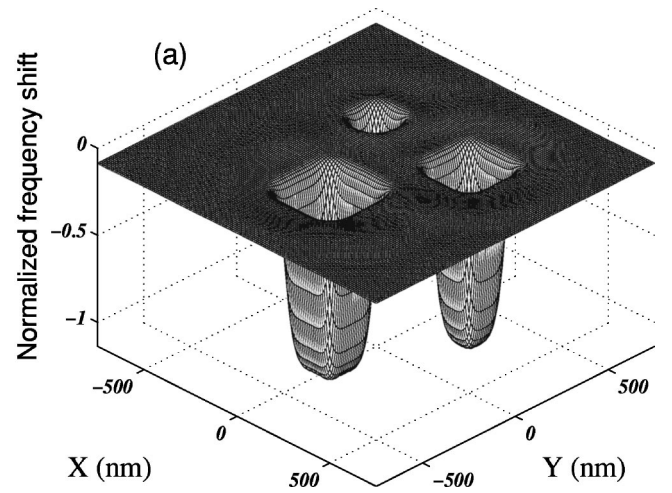

FIG. 12. Same as Fig. 1(a) but for the normalized frequency shift $\Delta\omega/\Gamma_0$.

APPENDIX: FREQUENCY SHIFTS AND MULTILEVEL ATOM

In this paper we use a classical treatment of the interaction between the molecule and the field. As we mentioned, owing to the classical nature of the field linear susceptibility, this classical approach is, for the decay rate, equivalent to a quantum-electrodynamics calculation where the molecule would be represented as a two-level system [54]. Indeed, the normalized decay rates computed in this way are identical to those that would stem from a quantum-mechanical description, only their derivation in a classical framework is simpler for complex geometries. For a multilevel system, the principle of the calculation is the same, one merely needs to add the contributions from all the allowed transitions to the decay rate. The case of the frequency shifts is different, however. The difference lies in the fact that part of the level shift is purely quantum mechanical. Let us assume that the molecular polarizability for a level a has the form

$$\alpha^a_{\alpha\beta}(\omega) = \frac{2}{\hbar} \sum_n \frac{\omega_{na}\mu^{an}_\alpha \mu^{na}_\beta}{\omega^2_{na} - (\omega + i\eta)^2}. \tag{A1}$$

It can then be shown [30] that the shift for level a consists of the two contributions

$$\delta E^{\mathrm{vdW}}_a = -\frac{\hbar}{2\pi} \int_0^\infty S_{\alpha\beta}(\mathbf{r}_0,\mathbf{r}_0,i\xi)\alpha^a_{\alpha\beta}(i\xi)d\xi, \tag{A2}$$

$$\delta E^{RR}_a = -\sum_n \mu^{an}_\alpha \mu^{na}_\beta \operatorname{Re}[S_{\alpha\beta}(\mathbf{r}_0,\mathbf{r}_0,\omega_{an})]\theta(\omega_{an}), \tag{A3}$$

where θ is the usual Heaviside step function. The first term (van der Waals or Casimir-Polder according to whether or not retardation is included), pertains to the polarization of the

molecule by vacuum fluctuations (in the presence of the environment). This term has no classical analog. The second term, on the other hand, has an obvious classical interpretation. It corresponds to the shift induced by radiation reaction, i.e., the dispersive effect of the component of the field reflected back by the environment and in phase with the dipole (source) oscillations. Also, unlike the preceding contribution, the derivation of this term does not require an explicit form of the polarizability. In the case of a transition from an excited state a to the (stable) ground state b, the classical frequency shift is given by $\delta E_a^{RR}/\hbar$. Actually, to get a classical expression, this shift should be normalized to the free space

decay rate Γ_0 to yield, in the case of a two-level atom, the classical result (see Ref. [55])

$$\frac{\Delta\omega}{\Gamma_0} = -\frac{3}{4k_0^3}\mathrm{Re}[S_{zz}(\mathbf{r}_0,\mathbf{r}_0,\omega)], \tag{A4}$$

where a term $-\Gamma_0/(8\omega)$ negligible compared to 1 has been dropped out. Therefore, the classical shift can be calculated by simply computing the real part of the field susceptibility in the self-consistent procedure described in Sec. III. An example is provided in Fig. 12.

---

[1] K.H. Drexhage, J. Lumin. **1,2**, 693 (1970); K.H. Drexhage, *Progress in Optics XII*, edited by E. Wolf (North-Holland, Amsterdam, 1974), p. 163.

[2] C.K. Carniglia, L. Mandel, and K.H. Drexhage, J. Opt. Soc. Am. **62**, 479 (1972).

[3] R.R. Chance, A. Prock, and R. Silbey, J. Chem. Phys. **60**, 2184 (1974); **60**, 2744 (1974); Adv. Chem. Phys. **37**, 1 (1978).

[4] R.E. Kunz and W. Lukosz, J. Opt. Soc. Am. **67**, 1607 (1977); **67**, 1615 (1977); R.E. Kunz and W. Lukosz, Opt. Commun. **20**, 195 (1977); W. Lukosz, Phys. Rev. B **21**, 4814 (1980); **22**, 3030 (1980); J. Opt. Soc. Am. **71**, 744 (1981); W. Lukosz and M. Meier, Opt. Lett. **6**, 251 (1981); Ch. Fattinger and W. Lukosz, J. Lumin. **31,32**, 933 (1984); M. Lieberherr, Ch. Fattinger, and W. Lukosz, Surf. Sci. **189,190**, 954 (1987).

[5] E.M. Purcell, Phys. Rev. **69**, 681 (1946).

[6] S. Haroche, in *Fundamental Systems in Quantum Optics*, edited by J. Dalibard, J. M. Raimond, and J. Zinn-Justin (North-Holland, Amsterdam, 1992), pp. 767–940.

[7] P.W. Milonni, *The Quantum Vacuum* (Academic, San Diego, 1994).

[8] H. Chew, Phys. Rev. A **38**, 3410 (1988).

[9] H. Metiu, Prog. Surf. Sci. **17**, 153 (1984).

[10] P.T. Leung and T.F. George, Phys. Rev. B **36**, 4664 (1987).

[11] D. Barchiesi, T. Pagnot, C. Pieralli, and D. Van Labeke, Proc. SPIE **2384**, 90 (1995).

[12] W.L. Blacke and P.T. Leung, Phys. Rev. B **56**, 12 625 (1997).

[13] D. Pastré, P. Grossel, and M. Troyon, J. Phys. D **31**, 2718 (1998); Opt. Commun. **156**, 92 (1998).

[14] C. Henkel and V. Sandoghdar, Opt. Commun. **158**, 250 (1998).

[15] G. Parent, D. Van Labeke, and D. Barchiesi, J. Opt. Soc. Am. A **16**, 896 (1999).

[16] R.X. Bian, R.C. Dunn, X.S. Xie, and P.T. Leung, Phys. Rev. Lett. **75**, 4772 (1995).

[17] X.S. Xie and R.C. Dunn, Science **265**, 361 (1994).

[18] W.P. Ambrose, P.M. Goodwin, J.C. Martin, and R.A. Keller, Science **265**, 364 (1994).

[19] J.K. Trautman and J.J. Macklin, Chem. Phys. **205**, 221 (1996).

[20] C. Girard, O.J.F. Martin, and A. Dereux, Phys. Rev. Lett. **75**, 3098 (1995).

[21] L. Novotny, Appl. Phys. Lett. **69**, 3806 (1996).

[22] C. Hafner, *The Generalized Multipole Technique for Computational Electromagnetics* (Artech, Boston, 1990).

[23] R. Kopelman, K. Lieberman, A. Lewis, and W. Tan, J. Lumin. **48-49**, 871 (1991).

[24] E. Betzig and R.J. Chichester, Science **262**, 1422 (1993).

[25] S.K. Sekatskii and V.S. Letokhov, Appl. Phys. B: Lasers Opt. **63**, 525 (1996).

[26] A. Rahmani, P.C. Chaumet, F. de Fornel, and C. Girard, Phys. Rev. A **56**, 3245 (1997).

[27] A. Rahmani, Ph.D. thesis, Université de Bourgogne, France, 1998; A. Rahmani and F. de Fornel, *Emission Photonique en Espace Confiné* (Eyrolles, Paris, 2000).

[28] G.S. Agarwal, Phys. Rev. A **11**, 230 (1975).

[29] G.S. Agarwal, Phys. Rev. A **12**, 1475 (1975).

[30] J.M. Wylie and J.E. Sipe, Phys. Rev. A **30**, 1185 (1984); **32**, 2030 (1985).

[31] H. Nha and W. Jhe, Phys. Rev. A **54**, 3505 (1996).

[32] M.S. Yeung and T.K. Gustafson, Phys. Rev. A **54**, 5227 (1996).

[33] W.L. Barnes, J. Mod. Opt. **45**, 661 (1998).

[34] J. Dalibard, J. Dupont-Roc, and C. Cohen-Tannoudji, J. Phys. (Paris) **43**, 1617 (1982).

[35] C. Cohen-Tannoudji, J. Dupont-Roc, and G. Grynberg, *Introduction à l'Électrodynamique Quantique* (InterEdition, Paris, 1987), pp. 223, 354–358; English translation: *Photons and Atoms: Introduction to Quantum Electrodynamics* (Wiley-Interscience, New York, 1989).

[36] C. Cohen-Tannoudji, J. Dupont-Roc, and G. Grynberg, *Processus d'Interaction Entre Photons et Atomes* (InterEdition, Paris, 1988), complément A_{IV}; English translation: *Atom-Photon Interactions: Basic Processes and Applications* (Wiley-Interscience, New York, 1992).

[37] J.D. Jackson, *Classical Electrodynamics*, 2nd ed. (Wiley, New York, 1975), p. 395.

[38] I.S. Gradshteyn and I.M. Ryzhik, *Table of Integrals, Series and Products, Corrected and Enlarged Edition* (Academic, New York, 1980).

[39] A. Rahmani and Garnett W. Bryant, Opt. Lett. **25**, 433 (2000).

[40] E.M. Purcell and C.R. Pennypacker, Astrophys. J. **186**, 705 (1973).

[41] F. Hynne and R.K. Bullough, J. Phys. A **5**, 1272 (1972).

[42] A. Wokaun, J.P. Gordon, and P.F. Liao, Phys. Rev. Lett. **48**, 957 (1982).

[43] B.T. Draine, Astrophys. J. **333**, 848 (1988); B.T. Draine and P.J. Flatau, J. Opt. Soc. Am. A **11**, 1491 (1994).

[44] P.C. Chaumet, A. Rahmani, F. de Fornel, and J.P. Dufour, Phys. Rev. B **58**, 2310 (1998).

[45] R. Schmehl, B.M. Nebeker, and E.D. Hirleman, J. Opt. Soc. Am. A **14**, 3026 (1997).

[46] P.C. Chaumet and M. Nieto-Vesperinas, Phys. Rev. B **61**, 14 119 (2000).

[47] P. C. Chaumet and M. Nieto-Vesperinas, Opt. Lett. **25**, 1065 (2000).

[48] *Handbook of Optical Constants of Solids*, edited by E. D. Palik (Academic Press, New York, 1985).

[49] F. de Fornel, *Evanescent Waves*, Vol. 73 of *Springer Series in Optical Sciences* (Springer Verlag, Berlin, 2000).

[50] W.H. Weber and C.F. Eagen, Opt. Lett. **4**, 236 (1979).

[51] M. Born and E. Wolf, *Principles of Optics*, 6th ed. (Cambridge University Press, Cambridge, 1980).

[52] J. Michaelis, C. Hettich, J. Mlynek, and V. Sandoghdar, Nature (London) **405**, 325 (2000).

[53] G.S. Agarwal, Phys. Rev. Lett. **84**, 5500 (2000).

[54] For a discussion of level shifts for a two-level atom see G. Barton, J. Phys. B **7**, 2134 (1974), and Ref. [29].

[55] R.R. Chance, A. Prock, and R. Silbey, Phys. Rev. A **12**, 1448 (1975).